Published for SISSA by Springer

Received: *August 23, 2021*
Revised: *October 19, 2021*
Accepted: *October 20, 2021*
Published: *November 4, 2021*

Probing leptogenesis and pre-BBN universe with gravitational waves spectral shapes

Rome Samanta[a] **and Satyabrata Datta**[b]

[a] *CEICO, Institute of Physics of the Czech Academy of Sciences, Na Slovance 1999/2, 182 21 Prague 8, Czech Republic*
[b] *Saha Institute of Nuclear Physics, HBNI, 1/AF Bidhannagar, Kolkata 700064, India*

E-mail: romesamanta@gmail.com, satyabrata.datta@saha.ac.in

Abstract: On the frequency-amplitude plane, Gravitational Waves (GWs) from cosmic strings show a flat plateau at higher frequencies due to the string loop dynamics in standard radiation dominated post-inflationary epoch. The spectrum may show an abrupt upward or a downward trend beyond a turning point frequency f_*, if the primordial dark age prior to the Big Bang Nucleosynthesis (BBN), exhibits non-standard cosmic histories. We argue that such a spectral break followed by a rising GW amplitude which is a consequence of a post-inflationary equation of state ($\omega > 1/3$) stiffer than the radiation ($\omega = 1/3$), could also be a strong hint of a leptogenesis in the seesaw model of neutrino masses. Dynamical generation of the right handed (RH) neutrino masses by a gauged U(1) symmetry breaking leads to the formation of a network of cosmic strings which emits stochastic GWs. A gravitational interaction of the lepton current by an operator of the form $\partial_\mu R j^\mu$ — which can be generated in the seesaw model at the two-loop level through RH neutrino mediation, naturally seeks a stiffer equation of state to efficiently produce baryon asymmetry proportional to $1-3\omega$. We discuss how GWs with reasonably strong amplitudes complemented by a neutrino-less double beta decay signal could probe the onset of the most recent radiation domination and lightest RH neutrino mass at the intermediate scales.

Keywords: Cosmology of Theories beyond the SM, CP violation, Neutrino Physics

ArXiv ePrint: 2108.08359

https://doi.org/10.1007/JHEP11(2021)017

JHEP11(2021)017

Contents

JHEP11(2021)017

1 Introduction

Leptogenesis [1–7] is a simple mechanism to explain the observed baryon asymmetry of the universe [8]. The right handed (RH) heavy neutrinos which are introduced in the Standard Model (SM) to generate light neutrino masses (Type-I seesaw), decay CP asymmetrically to create lepton asymmetry which is then converted to baryon asymmetry via Sphaleron transition [9]. When it comes to the testability of leptogenesis, there are subtleties. If the heavy neutrino masses are not protected by any symmetry [10], it is quite natural to assume that they are hierarchical in nature like any other family of SM fermions. In that case, the lightest RH mass scale is bounded from below $M \gtrsim 10^9$ GeV [11]which is beyond the reach of the present collider experiments. Nonetheless, still the colliders and other low energy neutrino experiments can probe leptogenesis mechanisms that do not constitute hierarchical RH neutrinos — starting from $\mathcal{O}$(TeV) to $\mathcal{O}$(MeV) scale heavy neutrinos [12–15]. A shift of attention from the collider experiments to the Gravitational Waves (GWs) physics is not less interesting in terms of testing leptogenesis. Particularly, this new cosmic frontier, in which after the discovery of GWs from black hole mergers by LIGO and Virgo collaboration [16, 17], plenty of efforts are being made to detect primordial GWs from the Early Universe (EU) within a wide range of frequencies — starting from the Pulsar Timing Arrays (PTAs, $\sim$ nHz) to the LIGO($\sim$ 25Hz).

A network of cosmic strings [18–20] which is a generic consequence of breaking symmetries such as U(1), is one of the prominent sources of strong stochastic primordial gravitational waves which can be tested in a complementary way in most of the planned GW detectors. Numerical simulations based on the Nambu-Goto action [21, 22] indicate that cosmic string loops loose energy dominantly via GW radiation, if the underlying broken symmetry corresponds to a local gauge symmetry. In the context of seesaw, this sounds music to the ears, since such a gauge symmetry is $U(1)_{B-L}$ [23–25], breaking of which could be responsible for the dynamical generation of the heavy RH masses and hence the lepton number violation as well as creation of a network of cosmic strings. Having this set-up, there could be two categories to look for the GWs as a probe of leptogenesis. *Category A:* a scale separation between the RH masses and the typical Grand Unified Theory (GUT) scale ($\sim 10^{16}\,\text{GeV}$), imposed by seesaw perturbativity condition and the neutrino oscillation data [26] implies that residual symmetries like $U(1)_{B-L}$ protects the RH neutrinos to get mass at the GUT scale. Therefore, breaking of that symmetry at a later stage and consequent emission of GWs from cosmic strings are natural probes of the scale of leptogenesis. In this case, it is the amplitude (GW energy density normalised by the critical energy density) of the GWs that matters as a probe and this approach has been taken in refs. [27, 28]. *Category B:* to make the testability more robust, along with the amplitudes, one can associate leptogenesis also to the spectral shapes of the GWs [29, 30]. Cosmic string loops that originate and decay in the radiation domination, exhibit a flat plateau on the amplitude-frequency plane at the higher frequencies. This spectral shape may show an upward or a downward trend if something other than radiation dominates the energy density of the EU before the onset (T_*) of most recent radiation domination prior to the BBN ($T \sim 5\,\text{MeV}$) [31–33]. Such a non-standard cosmic history that is responsible for this spectral break which along with the GW amplitude, one aims to claim also as a probe, should therefore be a natural/well-motivated call from the perspective of leptogenesis. Two well-known scenarios in this context can be opted for. *Category B1:* a matter domination ($\omega = 0 < 1/3$) [34, 35]. *Category B2:* scenarios such as kination ($\omega = 1 > 1/3$) [36, 37]. For the former (latter), one finds a spectral break followed by a downward (upward) going GW amplitude [38–41]. Two leptogenesis mechanisms in the *Category B1* — a low-scale leptogenesis and a leptogenesis from ultralight primordial black holes ($M_{PBH} \lesssim 13g$) have been studied in ref. [29] and ref. [30] respectively. In this article, we discuss a scenario that falls in the *Category B2*, i.e., interpreting a flat then a spectral break followed by a rising GW amplitude as a signature of leptogenesis.

Note that, two crucial ingredients for this typical signal are of course cosmic string network itself and then a non-standard equation of state ($\omega = 1$ in our discussion). In the context of leptogenesis from decays [1], though the former is a natural consequence in the sense of *Category A* [27], a stiffer equation of state is not an indispensable criterion. However, in seesaw models, even when the Lagrangian is minimally coupled to gravity, through massive RH neutrino mediation one can generate an operator of the form $\partial_\mu R j^\mu / M^2$ at two-loop level [42–44] (see also refs. [28, 45] for a flavour generalisation and ref. [46] for a recent review), where R is the Ricci scalar and j^μ is the lepton current. This operator is a well-studied operator [47–50] with the corresponding mechanism dubbed as "gravitational

JHEP11(2021)017

lepto/baryogenesis" and produces final baryon asymmetry proportional to $\dot{R} \propto (1 - 3\omega)$. Interestingly, note now that two primary ingredients of the GW signal are also natural requirements to obtain non-zero lepton asymmetry, i.e., the symmetry breaking which gives rise to massive RH neutrinos (mediate in the loops [44]) as well as cosmic strings and then an equation of state $\omega \neq 1/3$ [51]. We shall discuss later on, that indeed a stiffer equation of state is needed to efficiently produce lepton asymmetry. Plateau amplitudes corresponding to $G\mu \lesssim 10^{-12}$ with G being the Newton constant and μ being the string tension, with a post LISA spectral break supplemented by a potential test in neutrino-less double beta decay experiments, make the scenario generally robust. The above introduction summarises the basic idea and the main results of this paper. The next sections are dedicated to a more detailed description and technicalities.

2 Gravitational waves from cosmic strings

Cosmic strings may originate as the fundamental or composite objects in string theory [52, 53] as well as topological defects from spontaneous symmetry breaking (SSB) when the vacuum manifold $\mathcal{M}$ has a non-trivial first homotopy group $\pi_1(\mathcal{M})$. A theory with spontaneous breaking of a U(1) symmetry exhibits string solution [19, 20], since $\pi_1(\mathcal{M}) = \mathbb{Z}$. An example of a field theory containing string like solution is a theory of U(1)-charged complex scalar field ϕ that in the context of seesaw could be a SM scalar singlet ϕ_{B-L} which is responsible for the dynamical generation of RH neutrino masses. After the formation, strings get randomly distributed in space and form a network of horizon-size long strings [54, 55] characterised by a correlation length $L = \sqrt{\mu/\rho_\infty}$, where μ — the string tension or energy per unit length is in general constant (however, e.g., in case of global strings [56] and recently introduced melting strings [57] $\mu \sim f(T)$) and typically taken to be the square of the symmetry breaking scale Λ_{CS} and ρ_∞ is the long string energy density. When two segments of long strings cross each other they inter-commute and form loops with a probability $P = 1$ [58] (exceptions [59]). A string network may interact strongly with thermal plasma and thereby its motion gets damped [60]. After the damping stops, the strings oscillate and enter a phase of scaling evolution that constitute two competing dynamics namely the stretching of the correlation length due to the cosmic expansion and fragmentation of the long strings into loops which oscillate independently and produce particle radiation or gravitational waves [61–63]. Out of these two competing dynamics, there is an attractor solution called the scaling regime [64–66] in which the characteristic length scales as $L \sim t$. This implies, for constant string tension, $\rho_\infty \propto t^{-2}$. Therefore, the network tracks any cosmological background energy density $\rho_{bg} \propto a^{-3(1+\omega)} \propto t^{-2}$ with the same equation of state and hence cosmic strings do not dominate the energy density of the universe like any other defects. The loops radiate GWs at a constant rate which sets up the time evolution of a loop of initial size $l_i = \alpha t_i$ as $l(\tilde{t}) = \alpha t_i - \Gamma G\mu(\tilde{t} - t_i)$, where $\Gamma \simeq 50$ [61, 63] and the initial loops size parameter $\alpha \simeq 0.1$ — a value preferred by numerical simulations [67, 68]. The total energy loss from a loop is decomposed into a set of normal-mode oscillations with frequencies $f_k = 2k/l = a(t_0)/a(\tilde{t})f$, where $k = 1, 2, 3 \ldots k_{\max}$ ($k_{\max}$ is for numerical purpose, otherwise ∞) and f is the frequency observed today. Given

JHEP11(2021)017

the loop number density $n\left(\tilde{t}, l_k\right)$, the present time gravitational wave density parameter is given by $\Omega_{GW}(t_0, f) \equiv f\rho_c^{-1} d\rho_{GW}/df = \sum_k \Omega_{GW}^{(k)}(t_0, f)$, with the kth mode amplitude $\Omega_{GW}^{(k)}(t_0, f)$ as [67]

$$\Omega_{GW}^{(k)}(f) = \frac{2kG\mu^2\Gamma_k}{f\rho_c} \int_{t_{\rm osc}}^{t_0} \left[\frac{a(\tilde{t})}{a(t_0)}\right]^5 n\left(\tilde{t}, l_k\right) d\tilde{t}. \tag{2.1}$$

The quantity Γ_k depends on the small scale structures of the loop and is given by $\Gamma^{(k)} = \frac{\Gamma k^{-\delta}}{\zeta(\delta)}$, e.g., $\delta = 4/3$ and $5/3$ for cusps and kinks [69]. The integration in eq. (2.1) is subjected to a Heaviside function $\Theta \equiv \Theta(t_i - t_{\rm osc})\Theta(t_i - \frac{l_{cric}}{\alpha})$, with $t_{\rm osc} =$ Max [network formation time(t_F), end of damping$(t_{\rm fric})$] and l_{cric} is the critical length below which massive particle radiation dominates over GWs [70, 71]. Both these Θ functions set a high-frequency cut-off in the spectrum (a systematic analysis can be found in ref. [40]).

The most important aspect to obtain the GW spectrum is the computation of the loop number density $n\left(\tilde{t}, l_k\right)$ which we calculate from the Velocity-dependent-One-Scale (VOS) model [72–74] which assumes the loop production function to be a delta function, i.e. all the loops are created with the same fraction of the horizon size with a fixed value of α. Given a general equation of state parameter ω, the number density $n_\omega\left(\tilde{t}, l_k\right)$ is computed as

$$n_\omega(\tilde{t}, l_k(\tilde{t})) = \frac{A_\beta}{\alpha} \frac{(\alpha + \Gamma G\mu)^{3(1-\beta)}}{\left[l_k(\tilde{t}) + \Gamma G\mu\tilde{t}\right]^{4-3\beta}\, \tilde{t}^{3\beta}}, \tag{2.2}$$

where $\beta = 2/3(1+\omega)$ and we assume $A_\beta = 29.6$ $(\omega = 1), 5.4$ $(w = 1/3)$ and 0.39 $(\omega = 0)$ [74] is a step-function while changing the cosmological epochs. The most interesting feature of GWs from cosmic string is that the amplitude increases with the symmetry breaking scale Λ_{CS}. This can be seen by computing the $\Omega_{GW}^{(1)}$, considering loop production as well as decay in the radiation domination which gives an expression for a flat plateau at higher frequencies (see appendix A for an exact formula)

$$\Omega_{GW}^{(1)}(f) = \frac{128\pi G\mu}{9\zeta(\delta)} \frac{A_r}{\epsilon_r} \Omega_r \left[(1+\epsilon_r)^{3/2} - 1\right], \tag{2.3}$$

where $\epsilon_r = \alpha/\Gamma G\mu$ and $\Omega_r \simeq 9 \times 10^{-5}$. Such strong GWs as a consequence of a very high scale symmetry breaking thus serves as an outstanding probe of particle physics models [75–81]. Possibly the most important recent development is the finding of a stochastic common spectrum process across 45 pulsars by NANOGrav PTA [82], which if interpreted as GWs, corresponds to a strong amplitude and is better fitted with cosmic strings [28, 83, 84] than the single value power spectral density as predicted by supermassive black hole models. Let's also mention that a very recent analysis by PPTA [85] is in agreement with the NANOGrav result. In presence of an additional early kination era, the entire GW spectrum is determined by four dynamics. I) A peak at a lower frequency-caused by the loops which are produced in the radiation era and decay in the standard matter era. II) The flat plateau, $\Omega_{GW}^{\rm plt}$, as mention while describing eq. (2.3). III) A spectral break at $f_* = \sqrt{\frac{8}{\alpha\Gamma G\mu}} t_*^{-1/2} t_0^{-2/3} t_{\rm eq}^{1/6}$ — so called the turning point frequency [30, 39, 40], followed by a rising GW amplitude $\Omega_{GW}^{(1)}(f > f_*) \simeq \Omega_{GW}^{\rm plt}\,(f/f_*)$,

JHEP11(2021)017

caused by modified redshifting of the GWs during kination era V) a second turning point frequency f_Δ after which the GWs amplitude falls, e.g, due to particle productions below $l < l_{cric} = \beta_m \frac{\mu^{-1/2}}{(\Gamma G \mu)^m}$, with $\beta_m \sim \mathcal{O}(1)$ and $m = 1, 2$ for loops with kinks or cusps [70, 71]. If the falling is caused due to thermal friction, then one needs to consider the damping of the smaller loops along with the long-string network for $t < t_{fric}$, discarding any GWs production by the smaller loops, i.e, the entire dynamics is completely frozen until t_{fric} [60]. In fact, in our computation we do not take into account any GWs produced from smaller loops prior to t_{fric} and consider that the falling is due to particle production which sets the high-frequency cut-off that is much more stronger (appears at lower frequencies) than the friction cut-off [40]. Note also that if the two turning-point frequencies are close to each other, potentially the GW detectors could see a small bump after the flat plateau with a peak amplitude $\simeq \Omega^{\rm plt}_{GW}\,(f_\Delta/f_*)$. Nevertheless, as we show in the next section that given a successful leptogenesis, the second turning point frequency as well as small bumps are most likely to be outside the frequency range of the GW detectors.

Before concluding the section, we note two important points. Firstly, the VOS model overestimates the number density of the loops by an order of magnitude compared to the numerical simulations [67]. This is due to the fact that VOS model considers all the loops are of same size at the production. However, there could be a distribution of α. Numerical simulation finds that only 10% of the energy of the long-string network goes to the large loops ($\alpha \simeq 0.1$) while the rest 90% goes to the highly boosted smaller loops that do not contribute to the GWs. This fact is taken into account by including a normalisation factor $\mathcal{F}_\alpha \sim 0.1$ in eq. (2.2) [74]. Secondly, the amplitude beyond f_* goes as f^1 even after taking into account high-k modes (see appendix A) unlike the case of an early matter domination where the same changes from $f^{-1} \to f^{-1/3}$ for cusps like structures [29, 30, 40].

3 Gravitational leptogenesis, results and discussion

The idea behind gravitational leptogenesis [48] is, a C and CP-violating operator $\mathcal{L}_{CPV} \sim b\partial_\mu R j^\mu \sim b\partial_\mu R \bar{\ell}\gamma^\mu \ell$ with b as a real effective coupling, corresponds to a chemical potential $\mu = b\dot{R}$ for the lepton number in the theory. Therefore, the normalised (by photon density $n_\gamma \sim T^3$) equilibrium lepton asymmetry (using standard Fermi-Dirac statistics with energies $E_\pm = E \pm \mu$) is given by $N^{eq}_{B-L} \sim \frac{b\dot{R}}{T}$. Interestingly, $\mathcal{L}_{CPV}$ can be generated in a UV framework using the seesaw Lagrangian even when it is minimally coupled to gravity (see e.g., ref. [43] for an in-depth discussion, sectionII of ref. [28] for a brief summary). As a computational insight, one calculates an effective $\ell\ell h$ vertex corresponding to the operator $\mathcal{L}_{CPV}$ using a conformally flat metric $g_{\mu\nu} = (1+h)\eta_{\mu\nu}$ with $R = -3\partial^2 h$, capitalising the fact that the coupling 'b' is independent of the choice of background. In seesaw model, a similar $\ell\ell h$ vertex that manifests the $\mathcal{L}_{CPV}$ operator, can be constructed at two-loop level, where the Higgs and the RH masses mediate the loops. Then simply comparing the coefficients of both the vertices up to linear order in h, the coupling b can be calculated in terms of the Yukawa coupling f (where, $f_{\alpha i}\bar{\ell}_{L\alpha}\tilde{H}N_{Ri}$ is the Yukawa interaction in seesaw, with $\ell_{L\alpha}$, H and N_R being the lepton doublet, Higgs and RH fields respectively) and RH

JHEP11(2021)017

neutrino masses M_i. The expression for the equilibrium asymmetry then reads

$$N^{eq}_{B-L} = \frac{\pi^2 \dot{R}}{36(4\pi)^4} \sum_{j>i} \frac{\mathrm{Im}\left[k^2_{ij}\right]}{\zeta(3) T M_i M_j} \ln\left(\frac{M_j^2}{M_i^2}\right), \tag{3.1}$$

where $k_{ij} = (f^\dagger f)_{ij}$. The above expression could be modulated by a factor $(M_j^2/M_i^2)^\gamma$, where $\gamma = 0, 1$. However, $\gamma = 0$ appears to be the most natural solution which can be calculated exactly [43, 44]. In any case, even if one considers $\gamma = 1$ or the 'hierarchical enhancement', tuning the complex part in k^2_{ij}, correct baryon asymmetry can always be reproduced. The most important part is, $N_{B-L} \propto \dot{R} \propto 1 - 3\omega$ which is still vanishing in radiation domination at high temperatures with SM-QCD thermodynamic potential [51]. Therefore, a general cosmological background other than radiation that is quite a natural call now, always stems a non-vanishing equilibrium asymmetry unless the Yukawa couplings are real or purely imaginary. In the EU, any dynamically produced lepton asymmetry tracks the N^{eq}_{B-L} if the interaction that causes the asymmetry production is strong enough. When the interaction rate becomes weaker (compared to the Hubble expansion), the asymmetry freezes out with the potential to reproduce correct baryon asymmetry $N_{B-L} \sim 6 \times 10^{-8}$ [8]. In seesaw model, $\Delta L = 2$ interactions [86] play this role. The general evolution equation that governs the entire dynamics is given by

$$\frac{dN_{B-L}}{dz} = -\left(\frac{\kappa}{z^p} + W_{\rm ID}\right)\left[N_{B-L} - \frac{\beta}{z^q}\right], \tag{3.2}$$

where $z = M_1/T$, $W_{\Delta L=2}(z) = \frac{\kappa}{z^p}$ with $p = \frac{5-3\omega}{2}$, $N^{eq}_{B-L} = \frac{\beta}{z^q}$ with $q = \frac{7+9\omega}{2}$ and $W_{\rm ID}$ represents the inverse decay $\ell H \to N_1$ rate. The parameters $\kappa \sim f_\kappa(m_i, M_1) z_*^{\frac{1}{2}(1-3\omega)}$ and $N^{eq}_{B-L} \propto \beta \sim f_\beta(m_i, M_1, \mathrm{Im}[f_{ij}])(1-3\omega) z_*^{\frac{3}{2}(3\omega-1)}$, where $z_* = M_1/T_*$ and m_i is the i-th light neutrino mass with $i = 1, 2, 3$. All the exact expressions can be found in appendix B. Before proceeding further, let us mention that we do not include the charged lepton flavour effects in this analysis for simplicity. Nonetheless, a systematic description with flavour issues can be found in ref. [45] along with a more finer description in ref. [28]. To proceed further, the process consists of two distinct temperature regimes. At a higher temperature $T_{\rm in} \sim \Lambda_{CS}$, as soon as the symmetry breaks, the RH neutrinos become massive and eq. (3.2) starts acting without $W_{\rm ID}$ which is negligible at this regime. In this gravitational leptogenesis scenario, typically, $z_{\rm in} (= M_1/T_{\rm in})$ can be constrained with so called weak field condition as $z_{\rm in} \geq \sqrt{M_1/\tilde{M}_{\rm pl}}$, where $\tilde{M}_{\rm pl}$ is the reduced Planck constant. Once the asymmetry freezes out, at the lower temperatures, it faces a washout by the inverse decays which are strongly active at $T \sim M_1$. The final asymmetry is therefore of the form $N^f_{B-L} = N^{G0}_{B-L} e^{-\int_0^\infty W_{\rm ID}(z) dz}$, where N^{G0}_{B-L} is the frozen out asymmetry after the system is done with $\Delta L = 2$ interaction, and the exponential term represents a late-time washout by the inverse decays. A general solution of eq. (3.2) is complicated and depends on the properties of *incomplete Gamma functions*. However, for $\omega = 1$, that corresponds to $p = 1$ and $q = 8$, a simpler solution can be obtained. We find the expression for the final asymmetry $N^f_{B-L}(z \to \infty)$ to be

$$N^f_{B-L} \simeq \frac{\kappa\beta}{8 z_{\rm in}^8} \mathrm{Exp}\left[-\frac{4K_1}{z_*}\right], \tag{3.3}$$

JHEP11(2021)017

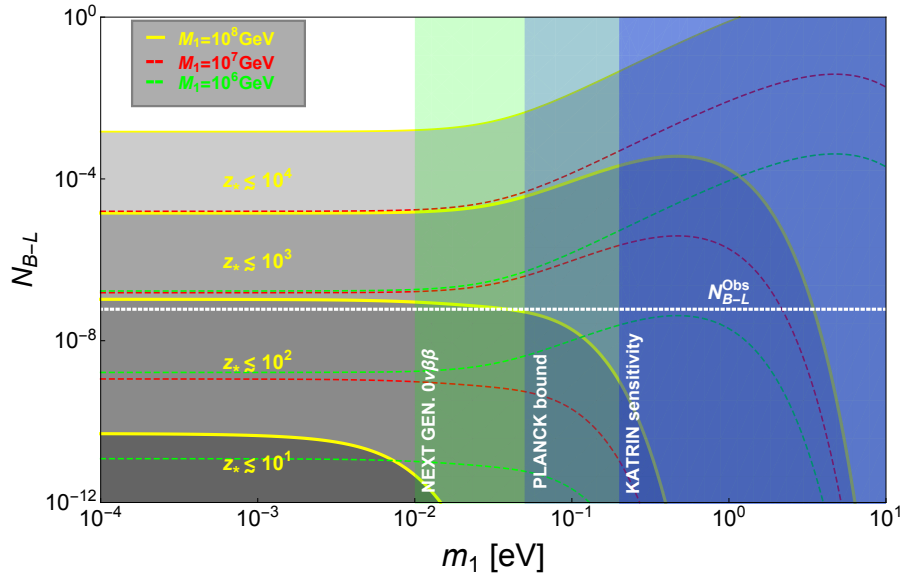

Figure 1. Eos: $\omega = 1$. The yellow, red and green lines correspond to the lightest RH mass $M_1 = 10^{8,7,6}\,\text{GeV}$. For $M_1 = 10^{7,6}$ we do not show the lines corresponding to $z_* = 10^1$. We take $M_3 = M_1/z_{\rm in}\,\text{GeV}$, $M_2 = 10^{-1}M_3\,\text{GeV}$, $x_{ij} = \pi/4$, $y_{ij} = 10^{-1}$ and two mass-squared differences are at their best-fit values.

where the dimensionless washout/decay parameter K_1 is a function of Yukawa couplings. Eq. (3.3) that matches with the numerical solutions of the eq. (3.2) with quite a high accuracy, is the master equation which we use to present all the results.

Prior to the explanation of figure 1, let's introduce a parametrisation of the Yukawa matrix as $m_D = U\sqrt{m}\Omega\sqrt{M}$, where $m_D = fv$ with $v = 174\,\text{GeV}$, U is the leptonic mixing matrix and Ω is a 3×3 complex orthogonal matrix with a standard parametrisation in terms of three complex rotation matrices [28] with complex angles $\theta_{ij} = x_{ij} + iy_{ij}$. In general, Ω is a completely 'free' matrix unless one invokes additional symmetries to fix the flavour structure of the theory. A plethora of works is dedicated in this direction [10]. With this orthogonal parametrisation it is easy to show that the equilibrium asymmetry is independent of U. Therefore, as far as the seesaw parameters are concerned, the light, heavy neutrino masses and the orthogonal matrix take part in the process. The decay parameter can also be expressed in terms of these parameters as $K_1 = m_*^{-1}\sum_k m_k|\Omega_{k1}|^2$ with $m_* \simeq 10^{-3}$ being the equilibrium neutrino mass [4]. In figure 1, we show the variation of the produced asymmetry with the lightest neutrino mass for three benchmark values; $M_1 = 10^{6,7,8}\,\text{GeV}$ with a fixed orthogonal matrix and different values of z_*. The basic nature of the curves is quite interesting. Let's focus on the $z_* = 10^3$ curve (yellow) for $M_1 = 10^8\,\text{GeV}$. It shows a plateau until $m_1 \simeq 10^{-2}\,\text{eV}$, then an increase followed by a downfall at large m_1 values. First of all, for $w = 1$, the parameter $\kappa \sim z_*^{-1}$ and therefore for large values of z_*, the strength of the $\Delta L = 2$ process becomes so weak that the asymmetry instantly freezes out without tracking the equilibrium number density. The coefficient f_κ does not change much until $m_1 \sim 10^{-2}\,\text{eV}$ and then increases for $m_1 \gtrsim 10^{-2}\,\text{eV}$ [28]. This increase in f_κ pushes the asymmetry more towards the equilibrium and hence the overall

JHEP11(2021)017

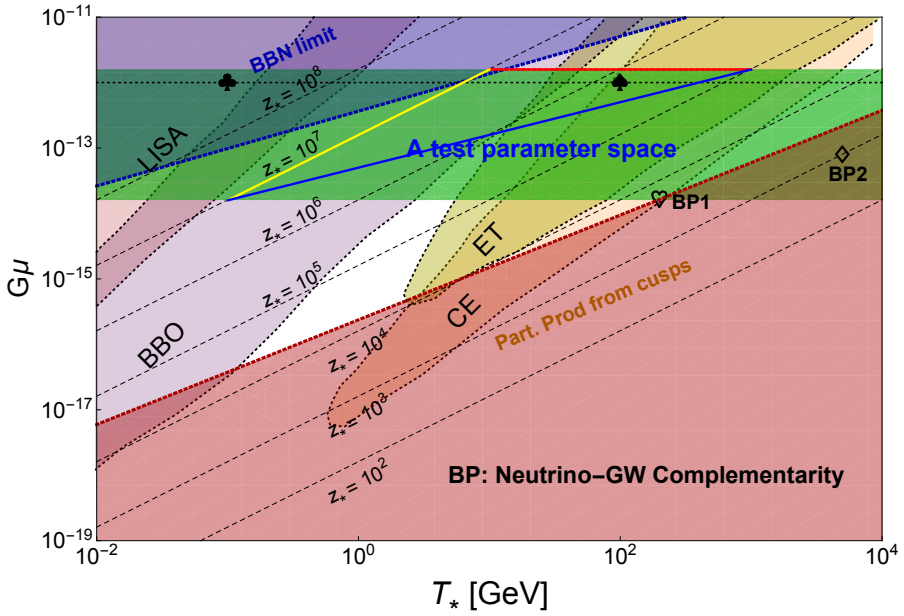

Figure 2. $G\mu$ vs. T_* plot against the sensitivities of various GW detectors.

magnitude of N_{B-L} increases for $m_1 \gtrsim 10^{-2}\,\text{eV}$. A downfall at large m_1 is caused by the exponential term in eq. (3.3). The washout is in fact modulated by two parameters, K_1 and z_*. However, for large values of m_1, the parameter K_1 becomes huge and therefore, even if one has a large z_*, the frozen out asymmetry is completely washed out. On the other hand, when z_* is small, e.g., $z_* = 10^2$, the overall magnitude of N_{B-L} decreases since $\beta \sim z_*^3$. In this case however, z_*^{-1} suppression in κ is not that significant compared to the previous one. Until $m_1 \sim 10^{-2}\,\text{eV}$, it shows the constant behaviour due to the mentioned nature of f_κ, however, at large m_1 values, it becomes strong enough to maintain the asymmetry in equilibrium for a period of time. The downfall is mostly dominated due to this equilibrium asymmetry tracking and not due to the late time washout. Note that for $\omega < 1/3$, for a fixed value of z_*, κ increases (causes delayed freeze out and hence dilution of the asymmetry N_{B-L}^{G0}) and β decreases (causes a decrease in N_{B-L}^{eq}). A concrete example is a matter domination, i.e., $\omega = 0$, where $\kappa \sim \sqrt{z_*}$ and $\beta \sim z_*^{-3/2}$. Moreover, these kind of scenarios are inclusive of a late time entropy production which dilutes the produced asymmetry significantly [30, 35]. Therefore, $\omega < 1/3$ scenarios are utterly inefficient. This possibly strengthens the claim that in the future, should the GW detectors find a flat and then a rising signal, RH neutrino induced gravitational leptogenesis with a stiffer equation of state is a natural mechanism to associate with, since both of them, successful leptogenesis and the GW signal, are triggered by common theoretical ingredients.

In figure 2, we show the future sensitivities of the GW detectors such as LISA [87], BBO [88], CE [89], ET [90] on the $G\mu - T_*$ plane. In the case of strong GW amplitudes, the most stringent constraint comes from the effective number of neutrino species which reads $\int df\, f^{-1}\Omega_{GW}(f)h^2 < 5.6 \times 10^{-6}\Delta N_{\text{eff}}$. Considering $\Delta N_{\text{eff}} \leq 0.2$, the peak of the spectrum at f_Δ, and taking into account contributions from the infinite number of modes that give

JHEP11(2021)017

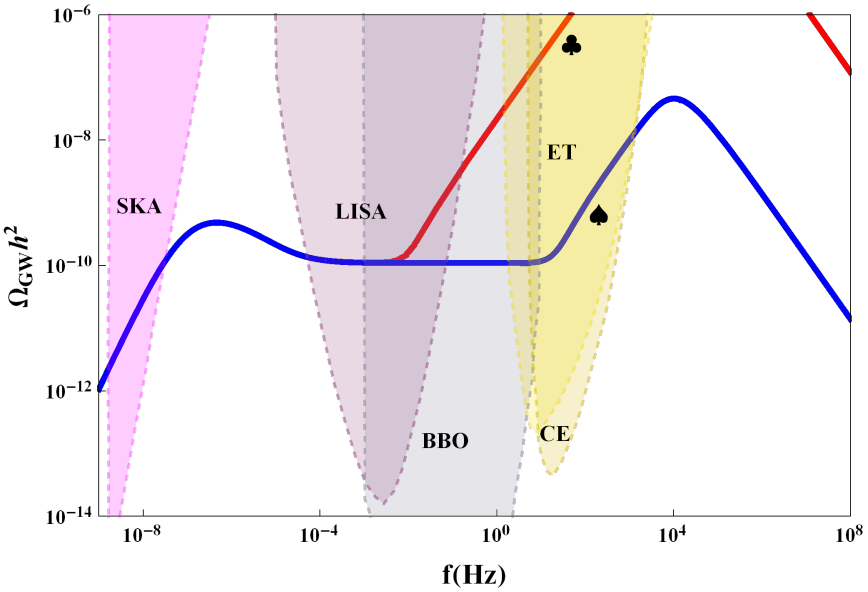

Figure 3. EOS: $\omega = 1$. The curve in blue (red) is a valid (invalid) signal of leptogenesis. The curves are generated with $G\mu = 10^{-12}$ and $T_* = 10^{-1}\,\text{GeV}$ (red) and $T_* = 10^{2}\,\text{GeV}$ (blue). A fall at a high frequency is due to the particle production from cusps for $l < l_{cric} = \frac{\mu^{-1/2}}{(\Gamma G\mu)^2}$ [40, 71]. We have shown the spectrum only for the fundamental mode.

a factor of $\zeta(7/3)$ amplification compared to the fundamental mode, the BBN constraint translates to $G\mu < T_*^{4/7}\left(1.72\times10^{-22}\right)^{4/7}$. This has been shown by the blue exclusion region. On the other hand, to observe two spectral breaks (at f_* and f_Δ) distinctly, one should have $f_\Delta > f_*$ which translates to the constraint $G\mu > T_*^{4/5}\left(2.88\times10^{-20}\right)^{4/5}$, where we consider particle production from cusps [71]. The corresponding region has been shaded in red. We have ignored the variation of the effective relativistic degrees of freedom even when T_* is below the QCD phase transition. Proper temperature dependence of the same, would include a factor of 1.5-3 modification. Since we are entirely onto the gravitational leptogenesis (to motivate $\omega \neq 1/3$), we take $M_1^{\max} \sim 10^8\,\text{GeV}$ so that the contribution from the decays are negligible. This gives an upper bound on the $T_{\text{in}}(\Lambda_{CS})$ that corresponds to $G\mu \lesssim 10^{-12}$. Therefore, the mechanism can be tested with reasonably strong GW amplitudes even for the flat part (eq. (2.3)). For strong amplitudes, the spectral breaks are likely to happen at high-frequency GW detectors like CE and ET plus the bump like signals (f_* and f_Δ are close to each other) in general lie outside those detectors. In figure 2, the black point represented by ♠ (♣), should (not) be a signal (see a supplementary figure 3).

We shall end the discussion with a 'Neutrino-Gravitational Waves Complementarity (NGWC)' or more generally, how this type of GW signal could be supplemented by low energy neutrino experiments. NGWC depends on the z_* and flavour structure of the theory or more precisely, on the orthogonal matrix. From figure 1, it can be seen that, depending on the RH neutrino mass (hence $G\mu$), various z_* values are sensitive to the neutrinoless double beta decay experiments (the N_{B-L} curves intersect with the N_{B-L}^{Obs} at the same time falls within the vertical green region). For the parameter set in figure 1, the NGWC

JHEP11(2021)017

points fall unfortunately in the red region as well as they are well outside the GW detectors (showed by the ♡ and ♢ points in figure 2). However, if one decreases the y_{ij}, to produce correct N_{B-L}, for a fixed value of $G\mu$ one needs larger values of z_*, meaning the NGWC points would move towards the left side, i.e., towards the smaller values of T_*. The entire picture can be encapsulated within the triangle drawn on the test parameter space shaded in green in figure 2. The red horizontal arm represents the constant $G\mu$ line along which the entries of Ω decrease as one goes from larger to smaller T_*. The yellow arm represents the constant z_* line, as one goes along the line towards smaller $G\mu$ values, entries of Ω increase and the blue arm represents the constant (already predicted) orthogonal matrix and as one goes towards the higher values of $G\mu$, z_* decreases or in other words, T_* increases. The blue arm is of great interest. If one has a completely determined orthogonal matrix, from figure 1 the NGWC points can be determined with the sets of M_1 and T_*. This means the blue arm is a line of predictions from the GW experiments, i.e., we can predict at which amplitude and at which frequency the spectral break would occur. The triangle as a whole can be pushed towards the larger T_* values increasing y_{ij}. This implies, seesaw models which exhibit an orthogonal matrix with large imaginary part entries, would likely to show the spectral break at higher frequencies and therefore may not be tested with the planned detectors. These models are dubbed as 'boosted' seesaw models where the light neutrino basis vectors and heavy neutrino basis vectors are strongly misaligned [91]. On the other hand, models with flavour structures close to 'form dominance' [92] that typically predicts a real orthogonal matrix ($\Omega = P$, where P is a permutation matrix), would show a spectral break within the frequency range of the current or planned GW detectors.

Acknowledgments

RS is supported by the MSCA-IF IV FZU - CZ.02.2.69/0.0/0.0/20_079/0017754 project and acknowledges European Structural and Investment Fund and the Czech Ministry of Education, Youth and Sports. RS acknowledges Graham M. Shore and Pasquale Di Bari for an useful discussion on gravitational leptogenesis and boosted seesaw models respectively, Kai Schmitz for a helpful chat on ref. [29] and Sabir Ramazanov for discussions on cosmic strings in general.

A Flat plateau, loop number density normalisation and the turning point frequencies

A.1 The standard expression

The normalised energy density parameter of gravitational waves at present time is expressed as

$$\Omega_{GW}(t_0, f) = \frac{f}{\rho_c}\frac{d\rho_{GW}}{df} = \sum_k \Omega^{(k)}_{GW}(t_0, f). \tag{A.1}$$

The frequency derivative of ρ_{GW} is given by

$$\frac{d\rho^{(k)}_{GW}}{df} = \int_{t_F}^{t_0} \left[\frac{a(\tilde{t})}{a(t_0)}\right]^4 P_{GW}(\tilde{t}, f_k)\frac{dF}{df}d\tilde{t}, \tag{A.2}$$

JHEP11(2021)017

where $\frac{dF}{df} = f\left[\frac{a(t_0)}{a(\tilde{t})}\right]$ the quantity $P_{GW}(\tilde{t}, f_k)$ represents the power emitted by the loops and is given by (see e.g., ref. [68])

$$P_{GW}(\tilde{t}, f_k) = G\mu^2\Gamma_k \int n(l, \tilde{t})\delta\left(f_k - \frac{2k}{l}\right) dl. \tag{A.3}$$

Integrating eq. (A.3) over the loop lengths gives

$$P_{GW}(\tilde{t}, f_k) = \frac{2kG\mu^2\Gamma_k}{f_k^2} n(\tilde{t}, f_k) = \frac{2kG\mu^2\Gamma_k}{f^2\left[\frac{a(t_0)}{a(\tilde{t})}\right]^2} n\left(\tilde{t}, \frac{2k}{f}\left[\frac{a(\tilde{t})}{a(t_0)}\right]\right). \tag{A.4}$$

From eq. (A.4) and eq. (A.2) one gets

$$\frac{d\rho_{GW}^{(k)}}{df} = \frac{2kG\mu^2\Gamma_k}{f^2} \int_{t_{\rm osc}}^{t_0} \left[\frac{a(\tilde{t})}{a(t_0)}\right]^5 n\left(\tilde{t}, \frac{2k}{f}\left[\frac{a(\tilde{t})}{a(t_0)}\right]\right) d\tilde{t} \tag{A.5}$$

and therefore the energy density corresponding to the mode 'k' is given by

$$\Omega_{GW}^{(k)}(t_0, f) = \frac{2kG\mu^2\Gamma_k}{f\rho_c} \int_{t_{\rm osc}}^{t_0} \left[\frac{a(\tilde{t})}{a(t_0)}\right]^5 n\left(\tilde{t}, \frac{2k}{f}\left[\frac{a(\tilde{t})}{a(t_0)}\right]\right) d\tilde{t}. \tag{A.6}$$

Using the VOS equations and considering the loop production function as a delta function (see, e.g., ref. [74]), it is easy to obtain the most general formula for the number density in an expanding background that scales as $a \sim t^\beta$. The expression is given by

$$n(\tilde{t}, l_k(\tilde{t})) = \frac{A_\beta}{\alpha} \frac{(\alpha + \Gamma G\mu)^{3(1-\beta)}}{\left[l_k(\tilde{t}) + \Gamma G\mu\tilde{t}\right]^{4-3\beta} \tilde{t}^{3\beta}}. \tag{A.7}$$

The eq. (A.6) can be expressed in the conventional form that are used in many papers (e.g., refs. [38, 39]) using the time dependence of the loop length which gives initial time $t_i^{(k)}$ as

$$t_i^{(k)} = \frac{l_k(\tilde{t}) + \Gamma G\mu\tilde{t}}{\alpha + \Gamma G\mu}, \tag{A.8}$$

Now using eq. (A.8), the number density in eq. (A.7) can be re-expressed as

$$n(\tilde{t}, l_k(\tilde{t})) = \frac{A_\beta(t_i^{(k)})}{\alpha(\alpha + \Gamma G\mu) t_i^{(k)4}} \left[\frac{a(t_i^k)}{a(\tilde{t})}\right]^3. \tag{A.9}$$

Putting the value of $n(\tilde{t}, l_k(\tilde{t}))$ from eq. (A.9) into eq. (A.6), one gets the standard expression

$$\Omega_{GW}^{(k)}(t_0, f) = \frac{2kG\mu^2\Gamma_k}{f\rho_c\alpha(\alpha + \Gamma G\mu)} \int_{t_{\rm osc}}^{t_0} \left[\frac{a(\tilde{t})}{a(t_0)}\right]^5 \frac{C_{\rm eff}(t_i^{(k)})}{t_i^{(k)4}} \left[\frac{a(t_i^k)}{a(\tilde{t})}\right]^3 d\tilde{t}, \tag{A.10}$$

where we have renamed A_β as $C_{\rm eff}$.

JHEP11(2021)017

A.2 The flat plateau

To obtain the GW spectrum from the loops that are produced and decay during the radiation domination, it is convenient to do the integration in eq. (A.6) with respect to the scale factor which reads

$$\Omega_{GW}^{(k)}(t_0,f)=\frac{16\pi}{3\zeta(\delta)}\left(\frac{G\mu}{H_0}\right)^2\frac{\Gamma}{fa(t_0)}\int_{a_*}^{a_{\rm eq}}H(a)^{-1}\left[\frac{a(\tilde{t})}{a(t_0)}\right]^4 n\left(\tilde{t},\frac{2k}{f}\left[\frac{a(\tilde{t})}{a(t_0)}\right]\right)da, \quad \text{(A.11)}$$

where

$$H=H_0\Omega_r^{1/2}\left(\frac{a(\tilde{t})}{a(t_0)}\right)^{-2} \quad \text{with} \quad \Omega_r\simeq 9\times 10^{-5}. \quad \text{(A.12)}$$

The number density $n\left(\tilde{t},l_k(\tilde{t})\equiv\frac{2k}{f}\left[\frac{a(\tilde{t})}{a(t_0)}\right]\right)$ in eq. (A.7) (in radiation domination) can also be expressed in terms of the scale factor as

$$n(\tilde{t},l_k(\tilde{t}))=\frac{A_r}{\alpha}\frac{(\alpha+\Gamma G\mu)^{3/2}}{\left[\frac{2}{f}\left[\frac{a(\tilde{t})}{a(t_0)}\right]+\Gamma G\mu/2H\right]^{5/2}(2H)^{-3/2}}. \quad \text{(A.13)}$$

Putting eq. (A.13) in eq. (A.11) and after performing the integration one gets

$$\Omega_{GW}^{(1)}(f)=\frac{128\pi G\mu}{9\zeta(\delta)}\frac{A_r}{\epsilon_r}\Omega_r(1+\epsilon_r)^{3/2}\left[\left(\frac{f}{f+\epsilon_r f_{\rm min}\left(\frac{t_*}{t_{\rm eq}}\right)^{1/2}}\right)^{3/2}-\left(\frac{f}{f+\epsilon_r f_{\rm min}}\right)^{3/2}\right], \quad \text{(A.14)}$$

where we define $\epsilon_r=\alpha/\Gamma G\mu$ the $f_{\rm min}=\frac{2}{\alpha t_*}\frac{a_*}{a_0}=\frac{4H_0\Omega_r^{1/2}}{\alpha}\frac{a_0}{a_*}$ is the minimum frequency emitted by a given loop. Given the scaling solution of the loop production rate, which decreases with the fourth power in time, $f\simeq f_{\rm min}$ is a reasonable assumption. Then, with $t_i\ll t_{\rm eq}$ one has

$$\Omega_{GW}^{(1)}(f)=\frac{128\pi G\mu}{9\zeta(\delta)}\frac{A_r}{\epsilon_r}\Omega_r\left[(1+\epsilon_r)^{3/2}-1\right]. \quad \text{(A.15)}$$

The expression for the flat plateau matches with ref. [74] barring the factor $\zeta(\delta)$ in the denominator. This is due to the fact that definition of the $\Omega_{GW}^{(k)}(f)$ in eq. (A.6) is inclusive of Γ^k.

A.3 The turning point frequencies

In the above, it is assumed that the dominant emission comes from the very earliest epoch of loop creation. Nonetheless, a precise value of the time can be calculated by maximizing the integral in eq. (A.11) with respect to $\tilde{t}$ which gives

$$\tilde{t}_M\simeq\frac{2}{f\Gamma G\mu}\frac{a_M}{a_0}\equiv\frac{1}{2\Gamma G\mu}\frac{4a_M}{fa_0}\equiv\frac{l_i}{2\Gamma G\mu}, \quad \text{(A.16)}$$

where f is the frequency observed today which was emitted at time $\tilde{t}_M$ when the a given initial loop $l_i=\alpha t_i$ reached to the half of its size $l_i/2$, i.e., $\tilde{t}_M$ is eventually the half-life of

JHEP11(2021)017

the loop. If time t_* at which the most recent radiation domination begins, an approximate frequency up to which the spectrum shows a flat plateau is given by

$$f_* = \sqrt{\frac{8}{\alpha\Gamma G\mu}} t_*^{-1/2} t_0^{-2/3} t_{\rm eq}^{1/6} \simeq \sqrt{\frac{8 z_{\rm eq}}{\alpha\Gamma G\mu}} \left(\frac{t_{\rm eq}}{t_*}\right)^{1/2} t_0^{-1}. \tag{A.17}$$

Similarly, using the critical length $l_{cric} = \frac{\mu^{-1/2}}{(\Gamma G\mu)^2}$ for cusp like structures, the second turning point frequency can be computed as

$$f_\Delta \simeq 9\sqrt{\alpha}\,(G\mu)^{5/4} \left(\frac{M_{\rm pl}}{T_*}\right) f_*, \tag{A.18}$$

where we have assumed that $f_\Delta/f_* \simeq \sqrt{t_*/t_\Delta}$ (cf. eq. (A.18)), and for simplicity we consider $g_*(T) = g_* \simeq 106$ throughout. Therefore, for post QCD phase transition $T \lesssim 200\,\text{MeV}$, the formula is bit errorful.

To observe both the frequencies distinctively, one should have $f_\Delta > f_*$. This gives the following restriction on the parameter space

$$G\mu > T_*^{4/5} \left(2.88 \times 10^{-20}\right)^{4/5} \tag{A.19}$$

which is shown by the red region in figure2.

A.4 The BBN limit

To be consistent with the number of effective neutrino species, the GW energy density has to comply with

$$\int_{f_{\rm BBN}}^{f_{\rm max}} \frac{df}{f} \Omega_{GW} h^2 < 5.6 \times 10^{-6} \Delta N_{\rm eff}, \tag{A.20}$$

with $\Delta N_{\rm eff} < 0.2$. Considering the dominant contribution from the non-flat part after the first turning point frequency f_*, the following constraint on the parameter space can be obtained

$$G\mu < T_*^{4/7} \left(1.22 \times 10^{-22}\right)^{4/7} \tag{A.21}$$

which is shown in the blue region in figure2. The constraints in eq. (A.19) and eq. (A.21) are derived for $\alpha = 0.1$.

A.5 Numerical simulation vs. VOS model loop number density and the normalisation

The number density obtained from numerical simulation is given by (see, ref. [68]) (considering the loops created during radiation domination)

$$n(\tilde{t}, l_k(\tilde{t})) = \frac{0.18}{\left[l_k(\tilde{t}) + \Gamma G\mu\tilde{t}\right]^{5/2} \tilde{t}^{3/2}}. \tag{A.22}$$

On the other hand considering the analytic approach, i.e., using Velocity dependent One Scale (VOS) the same is obtained as

$$n(\tilde{t}, l_k(\tilde{t})) = \frac{A_r}{\alpha} \frac{(\alpha + \Gamma G\mu)^{3/2}}{\left[l_k(\tilde{t}) + \Gamma G\mu\tilde{t}\right]^{5/2} \tilde{t}^{3/2}} \equiv \frac{A_r N_\alpha}{\left[l_k(\tilde{t}) + \Gamma G\mu\tilde{t}\right]^{5/2} \tilde{t}^{3/2}}, \tag{A.23}$$

JHEP11(2021)017

where $A_r = 5.4$. As mentioned before, the VOS model assumes all the loops are of same length at creation. However, at the moment of creation, the loops may follow a distribution depending on α. If so, the above formula should be modified as

$$n(\tilde{t}, l_k(\tilde{t})) = \frac{A_r \int w(\alpha) N_\alpha d\alpha}{\left[l_k(\tilde{t}) + \Gamma G \mu \tilde{t}\right]^{5/2} \tilde{t}^{3/2}}. \tag{A.24}$$

Therefore, to the make VOS formula in eq. (A.23) consistent with the numerical result, one has to normalise eq. (A.23), i.e.,

$$n(\tilde{t}, l_k(\tilde{t})) = \frac{\mathcal{F}_\alpha A_r N_\alpha}{\left[l_k(\tilde{t}) + \Gamma G \mu \tilde{t}\right]^{5/2} \tilde{t}^{3/2}}, \quad \text{with} \quad \mathcal{F}_\alpha = N_\alpha^{-1} \int w(\alpha) N_\alpha d\alpha \tag{A.25}$$

As one can see that for $\alpha = 0.1$, eq. (A.22) and eq. (A.23) is consistent for $\mathcal{F}_\alpha \sim 0.18/(A_r\sqrt{\alpha}) \sim 0.1$.

A.6 The spectral shape beyond the first turning point frequency

As mentioned previously in the main text, when the number of modes increases in the sum, the spectral behaviour beyond the turning point deviates from that of the fundamental mode (see e.g., refs. [29, 40]). The reason being the following:

from eq. (A.10) it is evident that

$$\Omega_{GW}(f) = \sum_k \Omega_{GW}^{(k)}(f) = \sum_k k^{-\delta} \Omega^{(1)}(f/k). \tag{A.26}$$

Now to perform the sum one can expand the r.h.s. of eq. (A.26) for some first few benchmark modes, i.e.,

$$\begin{aligned} \Omega_{GW}(f) &= \sum_k k^{-\delta} \Omega^{(1)}(f/k) \\ &= 1^{-\delta}\Omega^{(1)}(f/1) + m^{-\delta}\Omega^{(1)}(f/m) + n^{-\delta}\Omega^{(1)}(f/n) + r^{-\delta}\Omega^{(1)}(f/r) + \ldots, \end{aligned} \tag{A.27}$$

where the integers obey $1 < m < n < r$. This suggests, if one keeps on increasing the mode numbers, there should be a critical value $k \equiv k_*$ for which the amplitude $\Omega_{GW}^{(1)}(f_* = f/k_*)$ contributes to the frequency f. Therefore, the sum can be split into two parts. The first one is from $k = 1$ up to k_* for which the amplitude at f receives contributions from the non-flat part and the second one is from k_* to $k_{\rm max}$ for which the test point receives contribution from the flat part, i.e.,

$$\Omega_{GW}(f) = \sum_{k=1}^{k=k_*} k^{-\delta} \Omega_{GW}^{(1)}(f/k > f_*) + \sum_{k=k_*}^{k=k_{\rm max}} k^{-\delta} \Omega_{GW}^{(1)}(f/k < f_*) \tag{A.28}$$

$$= \sum_{k=1}^{k=k_*} k^{-\delta} \Omega_{GW}^{\rm plt}\left(\frac{f/k}{f_*}\right) + \sum_{k=k_*}^{k=k_{\rm max}} k^{-\delta} \Omega_{GW}^{\rm plt}. \tag{A.29}$$

The first term in eq. (A.29) gives the dominant contribution. In the large k_* limit, the sum is therefore

$$\Omega_{GW}(f) \simeq \Omega_{GW}^{\rm plt}\left(\frac{f}{f_*}\right) \sum_{k=1}^{k=k_*} k^{-(\delta+1)} \simeq \Omega_{GW}^{\rm plt}\left(\frac{f}{f_*}\right) \zeta(\delta+1). \tag{A.30}$$

Therefore, for an equation of states like kination, the spectral shape is quite similar to the $k = 1$ mode even after adding the contributions from the larger number of modes.

JHEP11(2021)017

B Evolution of the lepton asymmetry and derivation of the master equation

The energy density in a general equation of state red-shifts as $\rho_\omega \propto a^{-3(1+\omega)}$. We assume there is no further entropy production after the instantaneous reheating. Therefore the scale factor is inversely proportional to the temperature, i.e., $\rho_\omega \propto T^{3(1+\omega)}$. Since the energy density of radiation and field ϕ_ω should be equal at the critical temperature T_*, the proportionality constant σ_ω can then be obtained as

$$\sigma_\omega = \sigma_{\rm rad} T_*^{1-3\omega}, \tag{B.1}$$

where the energy density in radiation domination is given by $\rho_{\rm rad} = \sigma_{\rm rad} T^4 \equiv (\pi^2 g_*/30) T^4$. The total energy at an arbitrary temperature T is then given by

$$\rho(z) = \rho_{\rm rad}(z) \left[1 + \left(\frac{z}{z_*}\right)^{1-3\omega}\right], \tag{B.2}$$

where we define $z_*(z) = M_1/T_*(M_1/T)$. The modified Hubble parameter and the $\dot{R}$ in the general equation of state are then given by

$$H_\omega(z) = H_{\rm rad}(z) \left[1 + \left(\frac{z}{z_*}\right)^{1-3\omega}\right]^{1/2}, \tag{B.3}$$

$$\dot{R} = \sqrt{3}\sigma_{\rm rad}^{3/2}(1-3\omega)(1+w)\frac{T^6}{\tilde{M}_{\rm pl}^3}\left(\frac{z}{z_*}\right)^{\frac{3}{2}(1-3\omega)}. \tag{B.4}$$

Given the Hubble parameter in eq. (B.3), the expression for the lepton number violating interactions $W(z) \equiv \Gamma_{\Delta L=2}/Hz$ can be generalised as

$$W_\omega = W_{\rm rad} \left[1 + \left(\frac{z}{z_*}\right)^{1-3\omega}\right]^{-1/2}. \tag{B.5}$$

The most general Boltzmann equations (BEs) for leptogenesis with seesaw Lagrangian minimally coupled to gravity are

$$\frac{dN_{N_1}}{dz} = -D\left[N_{N_1} - N_{N_1}^{eq}\right], \tag{B.6}$$

$$\frac{\mathbf{dN_{B-L}}}{\mathbf{dz}} = -D\varepsilon_1\left[N_{N_1} - N_{N_1}^{eq}\right] - (\mathbf{W_{\Delta L=2}} + \mathbf{W_{ID}})\left[\mathbf{N_{B-L}} - \mathbf{N_{B-L}^{eq}}\right], \tag{B.7}$$

where the first equation governs the production of RH neutrinos and the first term in the second equation represents the contribution to the lepton asymmetry from RH neutrino decays. Since we are neglecting the contribution from decays, only the second equation with the terms in 'bold' is relevant. Note that recently in ref. [44], another curvature-induced evolution term that modulates of the asymmetry production dynamics at ultra-high temperatures has been introduced. We neglect that term in our computation. However, that will not change the qualitative features of our final results. To obtain a simpler form of the

JHEP11(2021)017

Boltzmann equation it is convenient to simplify the expression of the equilibrium asymmetry and the lepton number violating processes. Using the orthogonal parametrisation of the Dirac neutrino mass matrix $m_D = U\sqrt{m}\Omega\sqrt{M}$, the equilibrium asymmetry can be expressed as a power law in z as

$$N_{B-L}^{eq} = \frac{\beta}{z^q} \quad \text{with} \quad q = \frac{7+9\omega}{2}. \tag{B.8}$$

Here the parameter β is given by

$$\beta = \frac{\sqrt{3}\pi^2}{36(4\pi v)^4}\sigma_{\rm rad}^{3/2}(1-3\omega)(1+\omega)\frac{M_1^5}{\widetilde{M}_{\rm pl}^3}\mathcal{Y}, \tag{B.9}$$

where the parameter $\mathcal{Y}$ encodes CP violation in the theory and is given by

$$\mathcal{Y} = \sum_{j>i}\frac{\sum_{k,k'} m_k m_{k'} {\rm Im}\left[\Omega^*_{\rm ki}\Omega_{\rm kj}\Omega^*_{\rm k'i}\Omega_{\rm k'j}\right]}{\xi(3)}\ln\left(\frac{\rm M_j^2}{\rm M_i^2}\right) z_*^{\frac{3}{2}(3\omega-1)}. \tag{B.10}$$

In the $z_* \gg z$ limit, two relevant lepton number violating processes, i.e., $W_{\Delta L=2}$ scattering and the inverse decay $W_{\rm ID}$ can be obtained as

$$W_{\Delta L=2}(z) = \frac{\kappa}{z^p} \quad \text{with} \quad p = \frac{5-3\omega}{2}, \tag{B.11}$$

where κ depends on the M_1, the light neutrino masses and z_* as

$$\kappa = \frac{12 m^* M_1}{\pi^2 v^2}\left(\left[\frac{\sqrt{\sum_i m_i^2}}{m^*}\right]^2 + K_1^2 - \frac{2m_1^2}{m^{*2}}\right) z_*^{\frac{1}{2}(1-3\omega)} \tag{B.12}$$

and

$$W_{\rm ID}(z) \simeq \frac{1}{4}K_1 {z_*}^{-\frac{1}{2}(3\omega-1)} z^{\frac{7+3\omega}{2}-1}\mathcal{K}_1(z). \tag{B.13}$$

As mentioned earlier, at very high temperature the inverse decays are negligible. Therefore one can simply solve the BE

$$\frac{dN_{B-L}}{dz} = -\frac{\kappa}{z^p}\left[N_{B-L} - \frac{\beta}{z^q}\right] \tag{B.14}$$

to obtain the an expression for the frozen out asymmetry N_{B-L}^{G0}. Then the final asymmetry can be obtained as

$$N_{B-L}^{f} = N_{B-L}^{G0} e^{-\int_0^\infty W_{\rm ID}(z)dz}. \tag{B.15}$$

For $\omega = 1$, the solution for N_{B-L}^{G0} is obtained as

$$N_{B-L}^{G0} = \frac{\kappa\beta}{\kappa-8}\left(z^{-8} - z_{\rm in}^{\kappa-8} z^{-\kappa}\right) \tag{B.16}$$

which in the small κ and $z \gg z_{\rm in}$ limit simplifies as

$$N_{B-L}^{G0} = \frac{\kappa\beta}{8 z_{\rm in}^8}. \tag{B.17}$$

JHEP11(2021)017

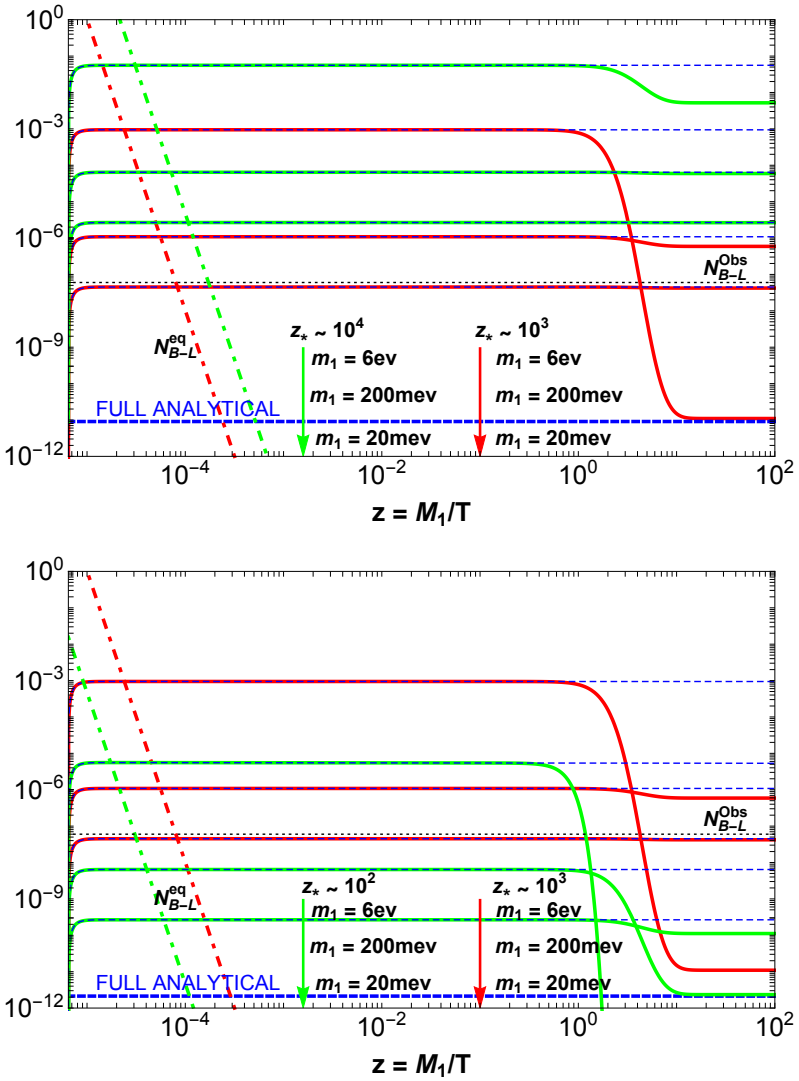

Figure 4. Top: EOS: $\omega = 1$. Evolution of the gravitationally produced asymmetry for different values of m_1. We have taken $M_1 = 10^8\,\text{GeV}$, $z_* = 1.3 \times 10^3$ (red), 10^4 (green) as benchmark values. Bottom: EOS: $\omega = 1$. Evolution of the gravitationally produced asymmetry for different values of m_1. We have taken $M_1 = 10^8\,\text{GeV}$, $z_* = 1.3 \times 10^3$ (red), 10^2 (green) as benchmark values. For both the plots we use $M_3 = 10^{14}\,\text{GeV}$, $M_2 = 10^{12}\,\text{GeV}$, $x_{ij} = \pi/4$, $y_{ij} = 10^{-4}$, $\Delta m^2_{12} = 7.4 \times 10^{-5}\text{eV}^2$, $\Delta m^2_{32} = 2.4 \times 10^{-3}\text{eV}^2$ and $z_{\text{in}} = \sqrt{M_1/\tilde{M}_{\text{pl}}}$. The thick blue dashed line shows a match bewteen numerical solutions and the master equation obtained in eq. (B.20). The thin blue dashed lines show a match bewteen numerical solutions and solution obtained (without the late time N_1-washout) in eq. (B.17).

JHEP11(2021)017

The washout by the inverse decays can be obtained using eq. (B.13) and integral properties of the Bessel function $\mathcal{K}_n(z)$

$$\int_0^\infty z^{\alpha-1}\mathcal{K}_n(z)dz = 2^{\alpha-2}\Gamma\left[\frac{\alpha-n}{2}\right]\Gamma\left[\frac{\alpha+n}{2}\right]. \tag{B.18}$$

The washout factor comes out as

$$e^{-\int_0^\infty W_{\rm ID}(z)dz} \equiv \mathcal{W}_{W_{\rm ID}(K_1,z_*,\omega=1)} = \text{Exp}\left[-\frac{4K_1}{z_*}\right]. \tag{B.19}$$

Therefore the master formula for the final asymmetry that can be used for a numerical scan is given by

$$N^f_{B-L} \simeq \frac{\kappa\beta}{8z^8_{\rm in}}\text{Exp}\left[-\frac{4K_1}{z_*}\right]. \tag{B.20}$$

which very accurately reproduces the numerical result as shown in figure4 with the phrase "FULL ANALYTICAL".

References

[1] M. Fukugita and T. Yanagida, *Baryogenesis without grand unification*, *Phys. Lett. B* **174** (1986) 45 [INSPIRE].

[2] A. Riotto and M. Trodden, *Recent progress in baryogenesis*, *Ann. Rev. Nucl. Part. Sci.* **49** (1999) 35 [hep-ph/9901362] [INSPIRE].

[3] A. Pilaftsis and T.E.J. Underwood, *Resonant leptogenesis*, *Nucl. Phys. B* **692** (2004) 303 [hep-ph/0309342] [INSPIRE].

[4] W. Buchmüller, P. Di Bari and M. Plümacher, *Leptogenesis for pedestrians*, *Annals Phys.* **315** (2005) 305 [hep-ph/0401240] [INSPIRE].

[5] S. Davidson, E. Nardi and Y. Nir, *Leptogenesis*, *Phys. Rept.* **466** (2008) 105 [arXiv:0802.2962] [INSPIRE].

[6] D. Bödeker and W. Buchmüller, *Baryogenesis from the weak scale to the grand unification scale*, *Rev. Mod. Phys.* **93** (2021) 035004 [arXiv:2009.07294] [INSPIRE].

[7] P. Di Bari, *On the origin of matter in the universe*, arXiv:2107.13750 [INSPIRE].

[8] Planck collaboration, *Planck* 2018 *results. X. Constraints on inflation*, *Astron. Astrophys.* **641** (2020) A10 [arXiv:1807.06211] [INSPIRE].

[9] V.A. Kuzmin, V.A. Rubakov and M.E. Shaposhnikov, *On the anomalous electroweak baryon number nonconservation in the early universe*, *Phys. Lett. B* **155** (1985) 36 [INSPIRE].

[10] G. Altarelli and F. Feruglio, *Discrete flavor symmetries and models of neutrino mixing*, *Rev. Mod. Phys.* **82** (2010) 2701 [arXiv:1002.0211] [INSPIRE].

[11] S. Davidson and A. Ibarra, *A lower bound on the right-handed neutrino mass from leptogenesis*, *Phys. Lett. B* **535** (2002) 25 [hep-ph/0202239] [INSPIRE].

JHEP11(2021)017

[12] E.K. Akhmedov, V.A. Rubakov and A.Y. Smirnov, *Baryogenesis via neutrino oscillations*, *Phys. Rev. Lett.* **81** (1998) 1359 [hep-ph/9803255] [INSPIRE].

[13] A. Pilaftsis and T.E.J. Underwood, *Resonant leptogenesis*, *Nucl. Phys. B* **692** (2004) 303 [hep-ph/0309342] [INSPIRE].

[14] T. Hambye and D. Teresi, *Higgs doublet decay as the origin of the baryon asymmetry*, *Phys. Rev. Lett.* **117** (2016) 091801 [arXiv:1606.00017] [INSPIRE].

[15] P.S. Bhupal Dev, P. Millington, A. Pilaftsis and D. Teresi, *Flavour covariant transport equations: an application to resonant leptogenesis*, *Nucl. Phys. B* **886** (2014) 569 [arXiv:1404.1003] [INSPIRE].

[16] LIGO Scientific and Virgo collaborations, *Observation of gravitational waves from a binary black hole merger*, *Phys. Rev. Lett.* **116** (2016) 061102 [arXiv:1602.03837] [INSPIRE].

[17] LIGO Scientific and Virgo collaborations, *GW*151226*: observation of gravitational waves from a* 22*-solar-mass binary black hole coalescence*, *Phys. Rev. Lett.* **116** (2016) 241103 [arXiv:1606.04855] [INSPIRE].

[18] T.W.B. Kibble, *Topology of cosmic domains and strings*, *J. Phys. A* **9** (1976) 1387 [INSPIRE].

[19] R. Jeannerot, J. Rocher and M. Sakellariadou, *How generic is cosmic string formation in SUSY GUTs*, *Phys. Rev. D* **68** (2003) 103514 [hep-ph/0308134] [INSPIRE].

[20] H.B. Nielsen and P. Olesen, *Vortex line models for dual strings*, *Nucl. Phys. B* **61** (1973) 45 [INSPIRE].

[21] C. Ringeval, M. Sakellariadou and F. Bouchet, *Cosmological evolution of cosmic string loops*, *JCAP* **02** (2007) 023 [astro-ph/0511646] [INSPIRE].

[22] J.J. Blanco-Pillado, K.D. Olum and B. Shlaer, *Large parallel cosmic string simulations: new results on loop production*, *Phys. Rev. D* **83** (2011) 083514 [arXiv:1101.5173] [INSPIRE].

[23] A. Davidson, $B - L$ *as the fourth color within an* $\mathrm{SU}(2)_L \times \mathrm{U}(1)_R \times \mathrm{U}(1)$ *model*, *Phys. Rev. D* **20** (1979) 776 [INSPIRE].

[24] R.E. Marshak and R.N. Mohapatra, *Quark-lepton symmetry and* $B - L$ *as the* U(1) *generator of the electroweak symmetry group*, *Phys. Lett. B* **91** (1980) 222 [INSPIRE].

[25] R.N. Mohapatra and R.E. Marshak, *Local* $B - L$ *symmetry of electroweak interactions, Majorana neutrinos and neutron oscillations*, *Phys. Rev. Lett.* **44** (1980) 1316 [*Erratum ibid.* **44** (1980) 1643] [INSPIRE].

[26] I. Esteban, M.C. Gonzalez-Garcia, M. Maltoni, T. Schwetz and A. Zhou, *The fate of hints: updated global analysis of three-flavor neutrino oscillations*, *JHEP* **09** (2020) 178 [arXiv:2007.14792] [INSPIRE].

[27] J.A. Dror, T. Hiramatsu, K. Kohri, H. Murayama and G. White, *Testing the seesaw mechanism and leptogenesis with gravitational waves*, *Phys. Rev. Lett.* **124** (2020) 041804 [arXiv:1908.03227] [INSPIRE].

[28] R. Samanta and S. Datta, *Gravitational wave complementarity and impact of NANOGrav data on gravitational leptogenesis*, *JHEP* **05** (2021) 211 [arXiv:2009.13452] [INSPIRE].

[29] S. Blasi, V. Brdar and K. Schmitz, *Fingerprint of low-scale leptogenesis in the primordial gravitational-wave spectrum*, *Phys. Rev. Res.* **2** (2020) 043321 [arXiv:2004.02889] [INSPIRE].

JHEP11(2021)017

[30] S. Datta, A. Ghosal and R. Samanta, *Baryogenesis from ultralight primordial black holes and strong gravitational waves from cosmic strings*, *JCAP* **08** (2021) 021 [arXiv:2012.14981] [INSPIRE].

[31] R.H. Cyburt, B.D. Fields, K.A. Olive and T.H. Yeh, *Big bang nucleosynthesis: present status*, *Rev. Mod. Phys.* **88** (2016) 015004.

[32] M. Kawasaki, K. Kohri and N. Sugiyama, *Cosmological constraints on late time entropy production*, *Phys. Rev. Lett.* **82** (1999) 4168 [astro-ph/9811437] [INSPIRE].

[33] T. Hasegawa, N. Hiroshima, K. Kohri, R.S.L. Hansen, T. Tram and S. Hannestad, *MeV-scale reheating temperature and thermalization of oscillating neutrinos by radiative and hadronic decays of massive particles*, *JCAP* **12** (2019) 012 [arXiv:1908.10189] [INSPIRE].

[34] M.S. Turner, *Coherent scalar field oscillations in an expanding universe*, *Phys. Rev. D* **28** (1983) 1243 [INSPIRE].

[35] K. Hamaguchi, H. Murayama and T. Yanagida, *Leptogenesis from N dominated early universe*, *Phys. Rev. D* **65** (2002) 043512 [hep-ph/0109030] [INSPIRE].

[36] L.H. Ford, *Gravitational particle creation and inflation*, *Phys. Rev. D* **35** (1987) 2955 [INSPIRE].

[37] P.J.E. Peebles and A. Vilenkin, *Quintessential inflation*, *Phys. Rev. D* **59** (1999) 063505 [astro-ph/9810509] [INSPIRE].

[38] Y. Cui, M. Lewicki, D.E. Morrissey and J.D. Wells, *Cosmic archaeology with gravitational waves from cosmic strings*, *Phys. Rev. D* **97** (2018) 123505 [arXiv:1711.03104] [INSPIRE].

[39] Y. Cui, M. Lewicki, D.E. Morrissey and J.D. Wells, *Probing the pre-BBN universe with gravitational waves from cosmic strings*, *JHEP* **01** (2019) 081 [arXiv:1808.08968] [INSPIRE].

[40] Y. Gouttenoire, G. Servant and P. Simakachorn, *Beyond the standard models with cosmic strings*, *JCAP* **07** (2020) 032 [arXiv:1912.02569] [INSPIRE].

[41] Y. Cui, M. Lewicki and D.E. Morrissey, *Gravitational wave bursts as harbingers of cosmic strings diluted by inflation*, *Phys. Rev. Lett.* **125** (2020) 211302 [arXiv:1912.08832] [INSPIRE].

[42] J.I. McDonald and G.M. Shore, *Radiatively-induced gravitational leptogenesis*, *Phys. Lett. B* **751** (2015) 469 [arXiv:1508.04119] [INSPIRE].

[43] J.I. McDonald and G.M. Shore, *Leptogenesis from loop effects in curved spacetime*, *JHEP* **04** (2016) 030 [arXiv:1512.02238] [INSPIRE].

[44] J.I. McDonald and G.M. Shore, *Dynamical evolution of gravitational leptogenesis*, *JHEP* **10** (2020) 025 [arXiv:2006.09425] [INSPIRE].

[45] R. Samanta and S. Datta, *Flavour effects in gravitational leptogenesis*, *JHEP* **12** (2020) 067 [arXiv:2007.11725] [INSPIRE].

[46] G.M. Shore, *A model of gravitational leptogenesis*, arXiv:2106.09562 [INSPIRE].

[47] A.G. Cohen and D.B. Kaplan, *Thermodynamic generation of the baryon asymmetry*, *Phys. Lett. B* **199** (1987) 251 [INSPIRE].

[48] H. Davoudiasl, R. Kitano, G.D. Kribs, H. Murayama and P.J. Steinhardt, *Gravitational baryogenesis*, *Phys. Rev. Lett.* **93** (2004) 201301 [hep-ph/0403019] [INSPIRE].

JHEP11(2021)017

[49] S. Mohanty, A.R. Prasanna and G. Lambiase, *Scale invariant leptogenesis from spin-gravity coupling following inflation*, *Phys. Rev. Lett.* **96** (2006) 071302 [gr-qc/0508037] [INSPIRE].

[50] G. Lambiase, S. Mohanty and A.R. Prasanna, *Neutrino coupling to cosmological background: a review on gravitational baryo/leptogenesis*, *Int. J. Mod. Phys. D* **22** (2013) 1330030 [arXiv:1310.8459] [INSPIRE].

[51] K. Saikawa and S. Shirai, *Primordial gravitational waves, precisely: the role of thermodynamics in the standard model*, *JCAP* **05** (2018) 035 [arXiv:1803.01038] [INSPIRE].

[52] E. Witten, *Cosmic superstrings*, *Phys. Lett. B* **153** (1985) 243 [INSPIRE].

[53] G. Dvali and A. Vilenkin, *Formation and evolution of cosmic D strings*, *JCAP* **03** (2004) 010 [hep-th/0312007] [INSPIRE].

[54] M.B. Hindmarsh and T.W.B. Kibble, *Cosmic strings*, *Rept. Prog. Phys.* **58** (1995) 477 [hep-ph/9411342] [INSPIRE].

[55] A. Vilenkin and E.P.S. Shellard, *Cosmic strings and other topological defects*, Cambridge University Press, Cambridge, U.K. (2000).

[56] C.-F. Chang and Y. Cui, *Gravitational waves from global cosmic strings and cosmic archaeology*, arXiv:2106.09746 [INSPIRE].

[57] W.T. Emond, S. Ramazanov and R. Samanta, *Gravitational waves from melting cosmic strings*, arXiv:2108.05377 [INSPIRE].

[58] E.P.S. Shellard, *Cosmic string interactions*, *Nucl. Phys. B* **283** (1987) 624 [INSPIRE].

[59] E.J. Copeland, T.W.B. Kibble and D.A. Steer, *Constraints on string networks with junctions*, *Phys. Rev. D* **75** (2007) 065024 [hep-th/0611243] [INSPIRE].

[60] A. Vilenkin, *Cosmic string dynamics with friction*, *Phys. Rev. D* **43** (1991) 1060 [INSPIRE].

[61] A. Vilenkin, *Gravitational radiation from cosmic strings*, *Phys. Lett. B* **107** (1981) 47 [INSPIRE].

[62] N. Turok, *Grand unified strings and galaxy formation*, *Nucl. Phys. B* **242** (1984) 520 [INSPIRE].

[63] T. Vachaspati and A. Vilenkin, *Gravitational radiation from cosmic strings*, *Phys. Rev. D* **31** (1985) 3052 [INSPIRE].

[64] D.P. Bennett and F.R. Bouchet, *Evidence for a scaling solution in cosmic string evolution*, *Phys. Rev. Lett.* **60** (1988) 257 [INSPIRE].

[65] D.P. Bennett and F.R. Bouchet, *Cosmic string evolution*, *Phys. Rev. Lett.* **63** (1989) 2776 [INSPIRE].

[66] A. Albrecht and N. Turok, *Evolution of cosmic string networks*, *Phys. Rev. D* **40** (1989) 973 [INSPIRE].

[67] J.J. Blanco-Pillado, K.D. Olum and B. Shlaer, *The number of cosmic string loops*, *Phys. Rev. D* **89** (2014) 023512 [arXiv:1309.6637] [INSPIRE].

[68] J.J. Blanco-Pillado and K.D. Olum, *Stochastic gravitational wave background from smoothed cosmic string loops*, *Phys. Rev. D* **96** (2017) 104046 [arXiv:1709.02693] [INSPIRE].

[69] T. Damour and A. Vilenkin, *Gravitational wave bursts from cusps and kinks on cosmic strings*, *Phys. Rev. D* **64** (2001) 064008 [gr-qc/0104026] [INSPIRE].

JHEP11(2021)017

[70] D. Matsunami, L. Pogosian, A. Saurabh and T. Vachaspati, *Decay of cosmic string loops due to particle radiation*, *Phys. Rev. Lett.* **122** (2019) 201301 [arXiv:1903.05102] [INSPIRE].

[71] P. Auclair, D.A. Steer and T. Vachaspati, *Particle emission and gravitational radiation from cosmic strings: observational constraints*, *Phys. Rev. D* **101** (2020) 083511 [arXiv:1911.12066] [INSPIRE].

[72] C.J.A.P. Martins and E.P.S. Shellard, *Quantitative string evolution*, *Phys. Rev. D* **54** (1996) 2535 [hep-ph/9602271] [INSPIRE].

[73] C.J.A.P. Martins and E.P.S. Shellard, *Extending the velocity dependent one scale string evolution model*, *Phys. Rev. D* **65** (2002) 043514 [hep-ph/0003298] [INSPIRE].

[74] P. Auclair et al., *Probing the gravitational wave background from cosmic strings with LISA*, *JCAP* **04** (2020) 034 [arXiv:1909.00819] [INSPIRE].

[75] W. Buchmüller, V. Domcke, H. Murayama and K. Schmitz, *Probing the scale of grand unification with gravitational waves*, *Phys. Lett. B* **809** (2020) 135764 [arXiv:1912.03695] [INSPIRE].

[76] S.F. King, S. Pascoli, J. Turner and Y.-L. Zhou, *Gravitational waves and proton decay: complementary windows into grand unified theories*, *Phys. Rev. Lett.* **126** (2021) 021802 [arXiv:2005.13549] [INSPIRE].

[77] B. Fornal and B. Shams Es Haghi, *Baryon and lepton number violation from gravitational waves*, *Phys. Rev. D* **102** (2020) 115037 [arXiv:2008.05111] [INSPIRE].

[78] W. Buchmüller, *Metastable strings and dumbbells in supersymmetric hybrid inflation*, *JHEP* **04** (2021) 168 [arXiv:2102.08923] [INSPIRE].

[79] W. Buchmüller, V. Domcke and K. Schmitz, *Stochastic gravitational-wave background from metastable cosmic strings*, arXiv:2107.04578 [INSPIRE].

[80] M.A. Masoud, M.U. Rehman and Q. Shafi, *Sneutrino tribrid inflation, metastable cosmic strings and gravitational waves*, arXiv:2107.09689 [INSPIRE].

[81] L. Bian, X. Liu and K.-P. Xie, *Probing superheavy dark matter with gravitational waves*, arXiv:2107.13112 [INSPIRE].

[82] NANOGrav collaboration, *The NANOGrav* 12.5 *yr data set: search for an isotropic stochastic gravitational-wave background*, *Astrophys. J. Lett.* **905** (2020) L34 [arXiv:2009.04496] [INSPIRE].

[83] J. Ellis and M. Lewicki, *Cosmic string interpretation of NANOGrav pulsar timing data*, *Phys. Rev. Lett.* **126** (2021) 041304 [arXiv:2009.06555] [INSPIRE].

[84] S. Blasi, V. Brdar and K. Schmitz, *Has NANOGrav found first evidence for cosmic strings?*, *Phys. Rev. Lett.* **126** (2021) 041305 [arXiv:2009.06607] [INSPIRE].

[85] B. Goncharov et al., *On the evidence for a common-spectrum process in the search for the nanohertz gravitational-wave background with the Parkes Pulsar Timing Array*, arXiv:2107.12112 [INSPIRE].

[86] W. Buchmüller, P. Di Bari and M. Plümacher, *Cosmic microwave background, matter-antimatter asymmetry and neutrino masses*, *Nucl. Phys. B* **643** (2002) 367 [*Erratum ibid.* **793** (2008) 362] [hep-ph/0205349] [INSPIRE].

[87] LISA collaboration, *Laser Interferometer Space Antenna*, arXiv:1702.00786 [INSPIRE].

JHEP11(2021)017

[88] V. Corbin and N.J. Cornish, *Detecting the cosmic gravitational wave background with the big bang observer*, *Class. Quant. Grav.* **23** (2006) 2435 [gr-qc/0512039] [INSPIRE].

[89] LIGO SCIENTIFIC collaboration, *Exploring the sensitivity of next generation gravitational wave detectors*, *Class. Quant. Grav.* **34** (2017) 044001 [arXiv:1607.08697] [INSPIRE].

[90] B. Sathyaprakash et al., *Scientific objectives of Einstein telescope*, *Class. Quant. Grav.* **29** (2012) 124013 [*Erratum ibid.* **30** (2013) 079501] [arXiv:1206.0331] [INSPIRE].

[91] P. Di Bari, M. Re Fiorentin and R. Samanta, *Representing seesaw neutrino models and their motion in lepton flavour space*, *JHEP* **05** (2019) 011 [arXiv:1812.07720] [INSPIRE].

[92] M.-C. Chen and S.F. King, *A_4 see-saw models and form dominance*, *JHEP* **06** (2009) 072 [arXiv:0903.0125] [INSPIRE].

JHEP11(2021)017